Position Control of a Two-Bar Linkage with Acceleration-Based Identification and Feedback

Jaganath Chandrasekar and Dennis S. Bernstein

I. Introduction

Kinematically complex mechanisms such as linkages with rigid members have been widely studied for centuries [1], and have numerous applications in areas such as robotics [2]. The dynamics of these systems are approximately linear for small amplitudes, but are strongly nonlinear for large motions [3].

The control of linkages encompasses the field of robotics [4, 5] and includes methods for controlling linkages that arise in specialized applications [6]. For large motions, the control of linkages represents a nonlinear control problem that has been addressed by a variety of techniques including PID control [7], feedback linearization [8, 9], and sliding mode methods [10]. These joint-space control methods tend to be computationally intensive since they require the solution of forward or inverse kinematics in real time. Alternatively, there exist task-space control techniques that do not require knowledge of the inverse kinematics [11, 12], although they require knowledge of the jacobian of the linkage. In addition, both methods generally assume that measurements of the displacement variables are available in real time.

For mechanisms whose kinematics or dynamics are uncertain, adaptive control methods have been used to account for uncertainty in physical parameters of the linkages and friction at the joints. These techniques assume a known structure for the dynamics and they combine estimation of the physical parameters of the linkage with feedback linearization techniques [13, 14]. Adaptive task-space control methods that account for uncertainty in the mass and lengths of the links, and the jacobian matrix have also been developed [15]. These methods also generally assume that measurements of the displacement variables of the critical members are available for feedback.

In many applications, however, measurements of the linkage displacements are not available. For example, for a Stewart platform it is generally difficult to determine the attitude of the platform from measurements of the joint angles due to uncertainty in the linkage geometry. Consequently, vision-based methods are proposed in [16] to determine the orientation of the platform.

In the present paper we propose the use of inertial sensors in combination with system identification methods to develop a model of the compliance transfer function that can be used for position-following control of a linkage. The inertial sensors are used off-line to develop the compliance model and on-line as signals for feedback. The advantage of this approach is that inertial sensors such as accelerometers and gyros are less expensive than position sensors. However, the method is limited to small amplitude motion with control accuracy limited by the fidelity of the identified transfer functions.

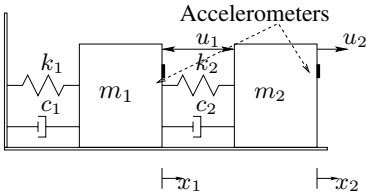

Fig. 1. Two-Mass System

Although only accelerometer and gyro measurements are assumed to be available, a state observer can be constructed to estimate position as long as the system has asymptotically stable dynamics and a model of the system is available. Asymptotically stable dynamics can be attained by using a preliminary PID control loop. To obtain a compliance model of the system, we use the available measurements in conjunction with subspace identification methods [17].

The goal of this paper is to present the procedure and demonstrate conceptually that position-following control based on inertial measurements is feasible. Experimental application to a 6-DOF Stewart manipulator will be given in a future paper.

II. Two-Mass System

Consider the two-mass system shown in Figure 1 with force inputs u_1, u_2 and two acceleration sensors (accelerometers) measuring $\ddot{x}_1$ and $\ddot{x}_2$. The equations of motion are

$$m_1\ddot{x}_1 + (c_1+c_2)\dot{x}_1 + (k_1+k_2)x_1 - c_2\dot{x}_2 - k_2x_2 = -u_1, \quad (2.1)$$

$$m_2\ddot{x}_2 + c_2\dot{x}_2 + k_2x_2 - c_2\dot{x}_1 - k_2x_1 = u_1 + u_2. \quad (2.2)$$

The state space representation of (2.1) and (2.2) is

$$\dot{x} = A_{\rm ct}x + B_{\rm ct}u, \quad (2.3)$$

where $x \in \mathbb{R}^4$ and $u \in \mathbb{R}^2$ are defined by

$$x \triangleq \begin{bmatrix} x_1 & x_2 & \dot{x}_1 & \dot{x}_2 \end{bmatrix}^{\rm T}, \; u \triangleq \begin{bmatrix} u_1 & u_2 \end{bmatrix}^{\rm T}, \quad (2.4)$$

This research was supported by the Air Force Office of Scientific Research under grant F429620-01-1-0094.

The authors are with Department of Aerospace Engineering, The University of Michigan, Ann Arbor, MI 48109-2140, (734) 764-3719, (734) 763-0578 (FAX), dsbaero@umich.edu

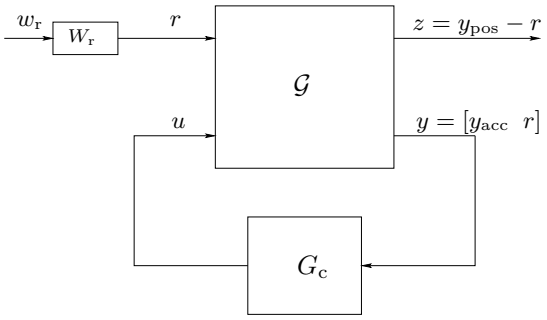

Fig. 2. Standard Problem for LQG design.

and $A_\mathrm{ct} \in \mathbb{R}^{4\times4}$ and $B_\mathrm{ct} \in \mathbb{R}^{4\times2}$ are defined by

$$A_\mathrm{ct} \triangleq \begin{bmatrix} 0 & 0 & 1 & 0 \\ 0 & 0 & 0 & 1 \\ -\frac{k_1+k_2}{m_1} & \frac{k_2}{m_1} & -\frac{c_1+c_2}{m_1} & \frac{c_2}{m_1} \\ \frac{k_2}{m_2} & -\frac{k_2}{m_2} & \frac{c_2}{m_2} & -\frac{c_2}{m_2} \end{bmatrix}, B_\mathrm{ct} \triangleq \begin{bmatrix} 0 & 0 \\ 0 & 0 \\ -\frac{1}{m_1} & 0 \\ \frac{1}{m_2} & \frac{1}{m_2} \end{bmatrix}^\mathrm{T}. \quad (2.5)$$

Define the acceleration y_acc and the position y_pos of the two masses by $y_\mathrm{acc} \triangleq \begin{bmatrix} \ddot{x}_1 & \ddot{x}_2 \end{bmatrix}^\mathrm{T}$, $y_\mathrm{pos} \triangleq \begin{bmatrix} x_1 & x_2 \end{bmatrix}^\mathrm{T}$, so that

$$y_\mathrm{acc} = C_\mathrm{acc}x + D_\mathrm{acc}u, \;\; y_\mathrm{pos} = C_\mathrm{pos}x, \quad (2.6)$$

where

$$\begin{aligned} C_\mathrm{acc} &\triangleq \begin{bmatrix} -\frac{k_1+k_2}{m_1} & \frac{k_2}{m_1} & -\frac{c_1+c_2}{m_1} & \frac{c_2}{m_1} \\ \frac{k_2}{m_2} & -\frac{k_2}{m_2} & \frac{c_2}{m_2} & -\frac{c_2}{m_2} \end{bmatrix}, \\ D_\mathrm{acc} &\triangleq \begin{bmatrix} -\frac{1}{m_1} & 0 \\ \frac{1}{m_2} & \frac{1}{m_2} \end{bmatrix}, C_\mathrm{pos} \triangleq \begin{bmatrix} 1 & 0 & 0 & 0 \\ 0 & 1 & 0 & 0 \end{bmatrix}. \end{aligned} \quad (2.7)$$

The systems with outputs y_pos and y_acc are the compliance and inertance, respectively.

The equivalent zero-order-hold discrete-time state space representation of (2.1) and (2.6) with sampling time t_s is

$$\begin{aligned} x(k+1) &= Ax(k) + Bu(k), \\ y_\mathrm{acc}(k) &= C_\mathrm{acc}x(k) + D_\mathrm{acc}u(k), \\ y_\mathrm{pos}(k) &= C_\mathrm{pos}x(k). \end{aligned} \quad (2.8)$$

Hence, the discrete-time inertance $G_\mathrm{inrt}(\mathbf{z})$ and discrete-time compliance $G_\mathrm{comp}(\mathbf{z})$ have realizations

$$G_\mathrm{comp}(\mathbf{z}) \sim \left[\begin{array}{c|c} A & B \\ \hline C_\mathrm{pos} & 0 \end{array}\right], G_\mathrm{inrt}(\mathbf{z}) \sim \left[\begin{array}{c|c} A & B \\ \hline C_\mathrm{acc} & D_\mathrm{acc} \end{array}\right]. \quad (2.9)$$

III. Acceleration-Based Position Control

The control objective is to have the positions x_1 and x_2 of the two masses follow a position reference command using only acceleration measurements y_acc. Define the position-error performance variable $\tilde{z}$ by $\tilde{z} \triangleq y_\mathrm{pos} - r$ and the plant output y by $y \triangleq \begin{bmatrix} y_\mathrm{acc}^\mathrm{T} & r^\mathrm{T} \end{bmatrix}^\mathrm{T}$, where $r \in \mathbb{R}^2$ is the position command to be followed. To facilitate LQG design, the position command r is represented as the output of a linear filter $W_\mathrm{r}(\mathbf{z})$ excited by a white noise signal w_r. Let $W_\mathrm{r}(\mathbf{z})$ have the minimal realization $W_\mathrm{r}(\mathbf{z}) \sim \left[\begin{array}{c|c} A_\mathrm{r} & B_\mathrm{r} \\ \hline C_\mathrm{r} & D_\mathrm{r} \end{array}\right]$ with state x_r. To include the control effort in the performance variable we define z by $z \triangleq \begin{bmatrix} \tilde{z}^\mathrm{T} & (Ru)^\mathrm{T} \end{bmatrix}^\mathrm{T}$, where the weighting $R \in \mathbb{R}^{2\times2}$ on the control input u is positive definite. We define w by $w \triangleq \begin{bmatrix} w_\mathrm{r}^\mathrm{T} & w_1^\mathrm{T} & w_2^\mathrm{T} \end{bmatrix}^\mathrm{T}$, where w_1 is zero-mean process noise on the state x and w_2 is zero-mean sensor noise that corrupts measurements y. It then follows from (2.8) that

$$\begin{bmatrix} z \\ y \end{bmatrix} = \mathcal{G} \begin{bmatrix} w \\ u \end{bmatrix}, \quad (3.1)$$

where $\mathcal{G}$ has the realization

$$\mathcal{G} \sim \left[\begin{array}{c|cc} \mathcal{A} & \mathcal{D}_1 & \mathcal{B} \\ \hline \mathcal{E}_1 & 0 & \mathcal{E}_2 \\ \mathcal{C} & \mathcal{D}_2 & \mathcal{D} \end{array}\right] \quad (3.2)$$

with state $\tilde{x} \triangleq \begin{bmatrix} x^\mathrm{T} & x_\mathrm{r}^\mathrm{T} \end{bmatrix}^\mathrm{T}$ and

$$\mathcal{A} \triangleq \begin{bmatrix} A & 0 \\ 0 & A_\mathrm{r} \end{bmatrix}, \mathcal{B} \triangleq \begin{bmatrix} B \\ 0 \end{bmatrix}, \mathcal{D}_1 = \begin{bmatrix} 0 & D_1 & 0 \\ B_\mathrm{r} & 0 & 0 \end{bmatrix}, \quad (3.3)$$

$$\mathcal{E}_1 \triangleq \begin{bmatrix} C_\mathrm{pos} & -C_\mathrm{r} \\ 0 & 0 \end{bmatrix}, \mathcal{E}_2 \triangleq \begin{bmatrix} 0 \\ R \end{bmatrix}, \quad (3.4)$$

$$\mathcal{C} \triangleq \begin{bmatrix} C_\mathrm{acc} & 0 \\ 0 & C_\mathrm{r} \end{bmatrix}, \mathcal{D} \triangleq \begin{bmatrix} D_\mathrm{acc} \\ 0 \end{bmatrix}, \mathcal{D}_2 \triangleq \begin{bmatrix} 0 & 0 & D_2 \\ D_\mathrm{r} & 0 & \varepsilon I \end{bmatrix}. \quad (3.5)$$

Since A_r is stable and (A, B) is controllable it follows from (3.3) that $(\mathcal{A}, \mathcal{B})$ is stabilizable. Furthermore, (A, C_acc) and $(A_\mathrm{r}, C_\mathrm{r})$ are observable, and hence it follows from (3.5) that $(\mathcal{A}, \mathcal{C})$ is also observable. To solve the estimator Riccati equation, we introduce εI in (3.5), where $\varepsilon > 0$ is small, so that $\mathcal{D}_2\mathcal{D}_2^\mathrm{T}$ is nonsingular.

The discrete-time LQG controller G_c can be obtained from the standard problem (3.2) by solving two discrete-time Riccati equations [18, 19]. Note that knowledge of the matrices A, B, C_acc, D_acc, and C_pos is required for LQG synthesis.

IV. Acceleration-Based Identification of the Compliance

We now assume that a model of the system is not available, although acceleration measurements can be used for system identification to obtain a model of the inertance. For system identification the force inputs u_1 and u_2 are chosen to be uncorrelated white noise signals, and the outputs are the acceleration measurement y_acc given by (2.8). A subspace identification algorithm [17] is used to obtain discrete-time system matrices A_id, B_id, $C_\mathrm{acc,id}$, and $D_\mathrm{acc,id}$ for the 4th-order linear time-invariant discrete-time state space inertance model

$$\begin{aligned} \hat{x}(k+1) &= A_\mathrm{id}\hat{x}(k) + B_\mathrm{id}u(k), \\ y_\mathrm{acc}(k) &= C_\mathrm{acc,id}\hat{x}(k) + D_\mathrm{acc,id}u(k). \end{aligned} \quad (4.1)$$

For LQG synthesis for position command following control, it is necessary to weight the position error. However, as a consequence of subspace identification, the components of $\hat{x}(k)$ do not have a physical interpretation. The state space models (2.8) and (4.1) represent the dynamics of the same system and hence the states x and $\hat{x}$ are related by a similarity transformation $x(k) = S\hat{x}(k)$ where $S \in \mathbb{R}^{4\times4}$ is nonsingular. Hence, it follows from (2.8) that $y_\mathrm{pos}(k) = \hat{C}_\mathrm{pos}\hat{x}(k)$, where $\hat{C}_\mathrm{pos} \triangleq C_\mathrm{pos}S$. However, S is unknown, and thus $\hat{C}_\mathrm{pos}$ cannot be determined analytically. Moreover, the position signal y_pos cannot be obtained by integrating the acceleration signal y_acc twice since a bias may be

present in $y_{\rm acc}$, and the initial position may be unknown. To overcome these difficulties, we construct a compliance model based on the inertance.

Let $\hat{G}_{\rm inrt}(\mathbf{z})$ be the identified inertance transfer function with realization

$$\hat{G}_{\rm inrt}(\mathbf{z}) \sim \left[\begin{array}{c|c} A_{\rm id} & B_{\rm id} \\ \hline C_{\rm acc,id} & D_{\rm acc,id} \end{array}\right]. \tag{4.2}$$

Next, consider the 2×2 discrete-time transfer function $G_{\rm dint}(\mathbf{z}) \triangleq \frac{t_{\rm s}^2}{(\mathbf{z}-1)^2} I_2$. Then, the compliance transfer function $\hat{G}_{\rm comp}(\mathbf{z})$ is defined by $\hat{G}_{\rm comp}(\mathbf{z}) \triangleq G_{\rm dint}(\mathbf{z})\hat{G}_{\rm inrt}(\mathbf{z})$. Let $G_{\rm dint}(\mathbf{z})$ have the 4th-order minimal realization

$$G_{\rm dint}(\mathbf{z}) \sim \left[\begin{array}{c|c} A_{\rm dint} & B_{\rm dint} \\ \hline C_{\rm dint} & 0 \end{array}\right], \tag{4.3}$$

with state $x_{\rm dint} \in \mathbb{R}^4$. It follows from (4.3) and (4.2) that $\hat{G}_{\rm comp}(\mathbf{z})$ has the 8th-order realization

$$\hat{G}_{\rm comp}(\mathbf{z}) \sim \left[\begin{array}{c|c} \hat{A}_{\rm comp} & \hat{B}_{\rm comp} \\ \hline \hat{C}_{\rm comp} & 0 \end{array}\right], \tag{4.4}$$

with state $\hat{x}_{\rm comp} \triangleq \left[\begin{array}{cc} \hat{x}^{\rm T} & x_{\rm dint}^{\rm T} \end{array}\right]^{\rm T}$, where

$$\hat{A}_{\rm comp} \triangleq \left[\begin{array}{cc} A_{\rm id} & 0_4 \\ B_{\rm dint}C_{\rm acc,id} & A_{\rm dint} \end{array}\right], \hat{B}_{\rm comp} \triangleq \left[\begin{array}{c} B_{\rm id} \\ B_{\rm dint}D_{\rm acc,id} \end{array}\right], \tag{4.5}$$

$$\hat{C}_{\rm comp} \triangleq \left[\begin{array}{cc} 0 & C_{\rm dint} \end{array}\right]. \tag{4.6}$$

It then follows from (4.1) that

$$y_{\rm acc}(k) = \left[\begin{array}{cc} C_{\rm acc,id} & 0 \end{array}\right] \hat{x}_{\rm comp}(k) + D_{\rm acc,id}u(k). \tag{4.7}$$

Note that all of the matrices in (4.5), (4.6), and (4.7) are known. However, the states $x_{\rm dint}$ of the double integrator are not observable through the acceleration measurement $y_{\rm acc}$, that is, $(\hat{A}_{\rm comp}, \left[\begin{array}{cc} C_{\rm acc,id} & 0 \end{array}\right])$ is not observable. Since the eigenvalues of $A_{\rm dint}$ are not observable, the realization $\hat{G}_{\rm comp}(\mathbf{z})$ is not convenient for LQG synthesis.

Instead, we determine an output matrix $\hat{C}_{\rm pos,id}$ so that $\hat{G}_{\rm comp}(\mathbf{z})$ has the minimal realization

$$\hat{G}_{\rm comp}(\mathbf{z}) \sim \left[\begin{array}{c|c} A_{\rm id} & B_{\rm id} \\ \hline \hat{C}_{\rm pos,id} & 0 \end{array}\right] \tag{4.8}$$

and the position $y_{\rm pos}$ is given by

$$y_{\rm pos}(k) = \hat{C}_{\rm pos,id}\hat{x}(k). \tag{4.9}$$

In particular, $\hat{C}_{\rm pos,id}$ is identified by comparing the Markov parameters of $\hat{G}_{\rm comp}(\mathbf{z})$ in (4.4) and (4.8). It follows from (4.4) and (4.8) that, for all $i \geqslant 1$,

$$\hat{C}_{\rm pos,id}A_{\rm id}^{i-1}B_{\rm id} = \hat{C}_{\rm comp}\hat{A}_{\rm comp}^{i-1}\hat{B}_{\rm comp}, \tag{4.10}$$

and hence $F = \hat{C}_{\rm pos,id}G$, where

$$\begin{aligned} F &\triangleq \left[\begin{array}{ccc} \hat{C}_{\rm comp}\hat{B}_{\rm comp} & \cdots & \hat{C}_{\rm comp}\hat{A}_{\rm comp}^5\hat{B}_{\rm comp} \end{array}\right], \\ G &\triangleq \left[\begin{array}{ccc} B_{\rm id} & \cdots & A_{\rm id}^5B_{\rm id} \end{array}\right]. \end{aligned} \tag{4.11}$$

The least squares fit is given by $\hat{C}_{\rm pos,id} = (G^{\dagger}F)^{\rm T}$.

V. Acceleration-Based Position Control Using the Identified Model

In this section we apply discrete-time LQG synthesis with the identified compliance and inertance models. Using (4.1) and (4.9), we consider (3.1)-(3.5) with A, B, $C_{\rm acc}$, $D_{\rm acc}$, and $C_{\rm pos}$ replaced by $A_{\rm id}$, $B_{\rm id}$, $C_{\rm acc,id}$, $D_{\rm acc,id}$, and $\hat{C}_{\rm pos,id}$, respectively. The standard problem for LQG synthesis is given by (3.2) with $\tilde{x}$ defined by $\tilde{x} \triangleq \left[\begin{array}{cc} \hat{x}^{\rm T} & x_{\rm r}^{\rm T} \end{array}\right]^{\rm T}$. The implementation of the controller is shown in Figure 3.

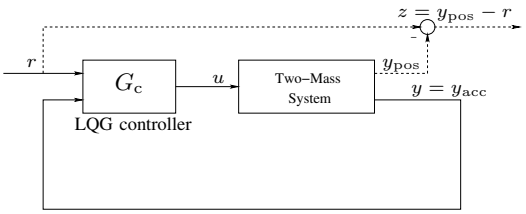

Fig. 3. Control architecture for discrete-time LQG position control of the two-mass system using acceleration feedback and identified inertance and compliance.

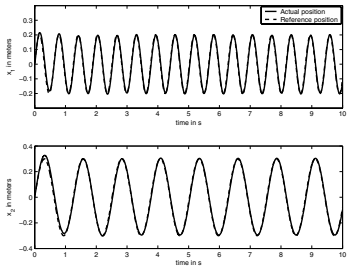

Fig. 4. Position command following for the LQG controller. The reference position command and the actual position of the two masses are shown by the dashed and bold lines, respectively.

To analyze the closed-loop dynamics, define $x_{\rm cl}$ by $x_{\rm cl} \triangleq \left[\begin{array}{cc} x^{\rm T} & x_{\rm c}^{\rm T} \end{array}\right]^{\rm T}$, where $x_{\rm c} \in \mathbb{R}^{n_{\rm c}}$ is the state of the controller $G_{\rm c}$ and x is defined in (2.4). Let $e \triangleq y_{\rm pos} - r$ be the error between the position command and the actual position of the two masses. The closed-loop system dynamics are then given by

$$\begin{aligned} x_{\rm cl}(k+1) &= A_{\rm cl}\tilde{x}(k) + B_{\rm cl}r(k), \\ e(k) &= C_{\rm cl}\tilde{x}(k) + D_{\rm cl}r(k), \end{aligned} \tag{5.1}$$

where

$$A_{\rm cl} \triangleq \left[\begin{array}{cc} A & BC_{\rm c} \\ B_{\rm c12}C_{\rm acc} & A_{\rm c} + B_{\rm c12}D_{\rm acc}C_{\rm c} \end{array}\right], B_{\rm cl} \triangleq \left[\begin{array}{c} 0 \\ B_{\rm c34} \end{array}\right], \tag{5.2}$$

$$C_{\rm cl} \triangleq \left[\begin{array}{cc} C_{\rm pos} & 0 \end{array}\right], \; D_{\rm cl} = -I \tag{5.3}$$

and $B_{\rm c} = \left[\begin{array}{cc} B_{\rm c12} & B_{\rm c34} \end{array}\right]$, where $B_{\rm c12} \in \mathbb{R}^{n_{\rm c}\times 2}$ and $B_{\rm c34} \in \mathbb{R}^{n_{\rm c}\times 2}$.

Let $G_{\rm sens}(\mathbf{z})$ be the sensitivity transfer function with the position command r as input, and the error e between the position command and actual position as the output. It then follows from (5.1)-(5.3) that $G_{\rm sens}(\mathbf{z})$ is realized by

$$G_{\rm sens}(\mathbf{z}) \sim \left[\begin{array}{c|c} A_{\rm cl} & B_{\rm cl} \\ \hline C_{\rm cl} & D_{\rm cl} \end{array}\right] \tag{5.4}$$

with SISO entries

$$G_{\rm sens}(\mathbf{z}) = \left[\begin{array}{cc} G_{{\rm sens}_{11}}(\mathbf{z}) & G_{{\rm sens}_{12}}(\mathbf{z}) \\ G_{{\rm sens}_{21}}(\mathbf{z}) & G_{{\rm sens}_{22}}(\mathbf{z}) \end{array}\right]. \tag{5.5}$$

To illustrate position-following control with acceleration-based identification and feedback, the two-mass system is simulated, and the inertance and

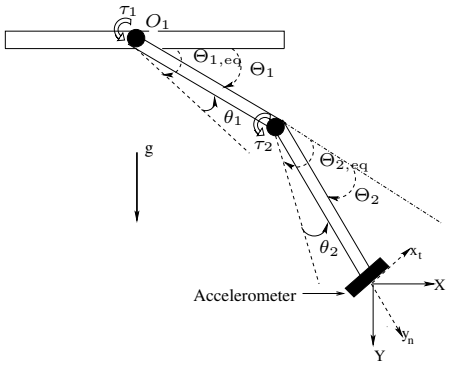

Fig. 5. Two-bar linkage with tip-mounted accelerometers

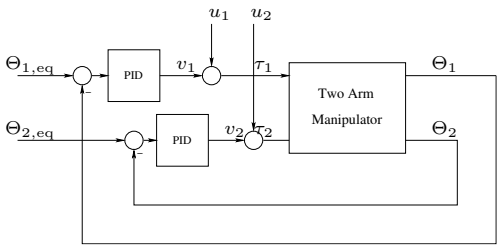

Fig. 6. Stabilization of the two-bar linkage using PID controllers

compliance transfer functions are identified as described in Section 4. The LQG controller is designed using the identified model. The position command and the actual positions of the two masses for the discrete-time LQG controller are shown in Figure 4.

VI. The Two-Bar Linkage

Consider the two-bar linkage shown in Figure 5. Assume the masses of the links are concentrated at their ends and the joints are frictionless. Let Θ_1 be the angle between the horizontal and the first link, and let Θ_2 be the angle between the first and the second link. Furthermore, assume that all angles measured in the counterclockwise direction are positive. Let τ_1 and τ_2 be the torque applied at the first and second joints, respectively. The equations of motion obtained from Lagrangian dynamics are then given by

$$M(\Theta_1,\Theta_2)\begin{bmatrix}\ddot{\Theta}_1\\ \ddot{\Theta}_2\end{bmatrix}+V(\Theta_1,\Theta_2,\dot{\Theta}_1,\dot{\Theta}_2)+G(\Theta_1,\Theta_2)=\tau, \quad (6.1)$$

where $M(\Theta_1,\Theta_2)\in\mathbb{R}^{2\times2}$, $V(\Theta_1,\Theta_2,\dot{\Theta}_1,\dot{\Theta}_2)\in\mathbb{R}^2$, $G(\Theta_1,\Theta_2)\in\mathbb{R}^2$ are defined in [4] and $\tau\triangleq\left[\begin{array}{cc}\tau_1 & \tau_2\end{array}\right]^{\mathrm{T}}$, and a_1 and a_2 are the lengths of the first and second links, respectively, and m_1 and m_2 are the masses of the two links. Note that, if $(\Theta_1,\Theta_2)\notin\{(\frac{\pi}{2},0),(-\frac{\pi}{2},0),(\frac{\pi}{2},\pi),(-\frac{\pi}{2},\pi)\}$ then (Θ_1,Θ_2) is not an equilibrium configuration. However, since measurements of the joint angles Θ_1 and Θ_2 are available, we use two PID controllers to stabilize the two-bar linkage at a specified equilibrium position $(\Theta_{1,\mathrm{eq}},\Theta_{2,\mathrm{eq}})$. To avoid a singular configuration, we assume that $\Theta_{2,\mathrm{eq}}\neq0$. The control architecture is shown in Figure 6.

Define $\Theta\in\mathbb{R}^4$ and $\Theta_{\mathrm{eq}}\in\mathbb{R}^4$ by

$$\Theta\triangleq\left[\begin{array}{cccc}\Theta_1 & \Theta_2 & \dot{\Theta}_1 & \dot{\Theta}_2\end{array}\right]^{\mathrm{T}},\ \Theta_{\mathrm{eq}}\triangleq\left[\begin{array}{cccc}\Theta_{1,\mathrm{eq}} & \Theta_{2,\mathrm{eq}} & 0 & 0\end{array}\right]^{\mathrm{T}}, \quad (6.2)$$

and define $\theta\in\mathbb{R}^4$ by $\theta\triangleq\Theta-\Theta_{\mathrm{eq}}$. Let $v=\left[\begin{array}{cc}v_1 & v_2\end{array}\right]^{\mathrm{T}}$ denote the output of the PID controller and let $u=\left[\begin{array}{cc}u_1 & u_2\end{array}\right]^{\mathrm{T}}$ be an external torque signal so that, for $i=1,2$, the total torque τ_i provided by the motor at joint i is given by $\tau_i=v_i+u_i$. Next, let $\eta=\left[\begin{array}{cc}\eta_1 & \eta_2\end{array}\right]^{\mathrm{T}}$ be the integrator states and let K_{P}, K_{I}, $K_{\mathrm{D}}\in\mathrm{R}^{2\times2}$ be the proportional, integrator, and derivative gains of the two PID controllers. We assume that K_P, K_I, and K_D are diagonal and in that case the dynamics of the PID controller are given by

$$\begin{aligned}\dot{\eta}&=\left[\begin{array}{cc}I_2 & 0_2\end{array}\right]\theta,\\ v&=-K_{\mathrm{I}}\eta+\left[\begin{array}{cc}-K_{\mathrm{P}} & -K_{\mathrm{D}}\end{array}\right]\theta.\end{aligned} \quad (6.3)$$

To analyze the augmented system consisting of the two-bar linkage and the two PID controllers, define $\theta_{\mathrm{aug}}\in\mathbb{R}^6$ by $\theta_{\mathrm{aug}}\triangleq\left[\begin{array}{cc}\eta & \theta\end{array}\right]^{\mathrm{T}}$. Substituting (6.2) into (6.1) and linearizing the resulting equation and (6.3) about $\theta_{\mathrm{aug}}=0$ yields the linear state space equation

$$\dot{\theta}_{\mathrm{aug}}=A_{\mathrm{jt}}\theta_{\mathrm{aug}}+B_{\mathrm{jt}}u, \quad (6.4)$$

where $A_{\mathrm{jt}}\in\mathbb{R}^{6\times6}$ and $B_{\mathrm{jt}}\in\mathbb{R}^{6\times2}$.

To design a position-following controller, we express the system dynamics in terms of Cartesian coordinates. Let (X_1,X_2) denote the position of the end effector with respect to the first joint O_1. Since the two-bar linkage operates in a small neighborhood of the equilibrium position, the relation between (X_1,X_2) and (Θ_1,Θ_2) is unique and determined by the forward kinematics (see [4]) given by

$$\left[\begin{array}{c}X_1\\ X_2\end{array}\right]=h(\Theta_1,\Theta_2), \quad (6.5)$$

where $h:\mathbb{R}^2\to\mathbb{R}^2$ is defined by

$$h(\Theta_1,\Theta_2)=\left[\begin{array}{c}a_1\cos\Theta_1+a_2\cos(\Theta_1+\Theta_2)\\ a_1\sin\Theta_1+a_2\sin(\Theta_1+\Theta_2)\end{array}\right]. \quad (6.6)$$

Linearizing (6.6) about $\Theta=\Theta_{\mathrm{eq}}$ and substituting (6.2) into the resulting equation yields

$$\left[\begin{array}{c}X_1\\ X_2\end{array}\right]=h(\Theta_{1,\mathrm{eq}},\Theta_{2,\mathrm{eq}})+J_0\left[\begin{array}{c}\theta_1\\ \theta_2\end{array}\right], \quad (6.7)$$

where the jacobian $J_0\in\mathbb{R}^{2\times2}$ of h at $(\Theta_1,\Theta_2)=(\Theta_{1,\mathrm{eq}},\Theta_{2,\mathrm{eq}})$ is nonsingular and given by

$$J_0=\frac{\partial h}{\partial(\Theta_1,\Theta_2)}\Big|_{(\Theta_{1,\mathrm{eq}},\Theta_{2,\mathrm{eq}})} \quad (6.8)$$

Next, define the relative position (x_1,x_2) by

$$\left[\begin{array}{c}x_1\\ x_2\end{array}\right]\triangleq\left[\begin{array}{c}X_1\\ X_2\end{array}\right]-h(\Theta_{1,\mathrm{eq}},\Theta_{2,\mathrm{eq}}) \quad (6.9)$$

and define $x\in\mathbb{R}^4$ by $x\triangleq\left[\begin{array}{cccc}x_1 & x_2 & \dot{x}_1 & \dot{x}_2\end{array}\right]$. Defining $x_{\mathrm{aug}}\in\mathbb{R}^6$ by $x_{\mathrm{aug}}\triangleq\left[\begin{array}{cc}\eta & x\end{array}\right]^{\mathrm{T}}$, it follows from (6.7)-(6.9) that $x_{\mathrm{aug}}=T\theta_{\mathrm{aug}}$, where $T\in\mathbb{R}^{6\times6}$ is defined by

$$T\triangleq\left[\begin{array}{ccc}I_2 & 0 & 0\\ 0 & J_0 & 0\\ 0 & 0 & J_0\end{array}\right]. \quad (6.10)$$

Hence it follows from (6.4) that

$$\dot{x}_{\mathrm{aug}}=A_{\mathrm{ct}}x_{\mathrm{aug}}+B_{\mathrm{ct}}u, \quad (6.11)$$

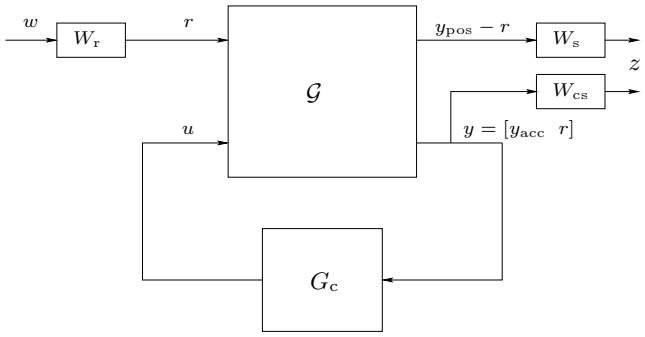

Fig. 7. Standard Problem for Mixed Weighted Sensitivity Minimization LQG design.

where $A_{\rm ct}$ and $B_{\rm ct}$ are defined by $A_{\rm ct} \triangleq TA_{\rm jt}T^{-1}$, $B_{\rm ct} \triangleq TB_{\rm jt}$. Next, define $C_{\rm acc}$, $D_{\rm acc}$, and $C_{\rm pos}$ so that the acceleration $y_{\rm acc} \triangleq \begin{bmatrix} \ddot{x}_1 & \ddot{x}_2 \end{bmatrix}$ and the position $y_{\rm pos} \triangleq \begin{bmatrix} x_1 & x_2 \end{bmatrix}$ can be expressed as

$$\begin{aligned} y_{\rm acc} &= C_{\rm acc}x_{\rm aug} + D_{\rm acc}u, \\ y_{\rm pos} &= C_{\rm pos}x_{\rm aug}. \end{aligned} \tag{6.12}$$

Next, let the zero-order-hold discrete-time equivalent of (6.11) and (6.12) be given by

$$\begin{aligned} x_{\rm aug}(k+1) &= Ax_{\rm aug}(k) + Bu(k), \\ y_{\rm acc}(k) &= C_{\rm acc}x_{\rm aug}(k) + D_{\rm acc}u(k), \\ y_{\rm pos}(k) &= C_{\rm pos}x_{\rm aug}(k). \end{aligned} \tag{6.13}$$

The control objective is to have the position $y_{\rm pos}$ of the end effector follow a position command using acceleration measurements. However, the accelerometers attached to the end effector provide measurements of the tangential and normal components $y_{\rm acc,n}$ and $y_{\rm acc,t}$ of the acceleration and not of the cartesian accelerations $y_{\rm acc}$. Assuming the two links are straight, it follows from the geometry of the two-bar linkage that

$$y_{\rm acc} = \begin{bmatrix} y_{\rm acc,n}\cos(\Theta_1+\Theta_2) - y_{\rm acc,t}\sin(\Theta_1+\Theta_2) \\ y_{\rm acc,n}\sin(\Theta_1+\Theta_2) + y_{\rm acc,t}\cos(\Theta_1+\Theta_2) \end{bmatrix}. \tag{6.14}$$

Since measurements of the angles Θ_1 and Θ_2 are available, $y_{\rm acc}$ can be evaluated online using (6.14).

The dynamics of the two-bar linkage involve the masses and lengths of the two links, which are unknown. Moreover, the nonlinear equations of motion (6.1) must be known in order to determine the matrices A, B, $C_{\rm acc}$, and $D_{\rm acc}$. To account for modeling limitations, torque and acceleration data are used to identify the discrete-time system matrices $A_{\rm id}$, $B_{\rm id}$, $C_{\rm acc,id}$, and $D_{\rm acc,id}$. Substituting the identified matrices $A_{\rm id}$, $B_{\rm id}$, $C_{\rm acc,id}$, $D_{\rm acc,id}$ into (4.5)-(4.11) yields $\hat{C}_{\rm pos,id}$. The identified inertance and compliance models are used to synthesize the position-following controller $G_{\rm c}$ by following the procedure described in Section 5. Note that knowledge of h in (6.6) and J_0 in (6.8) is not necessary.

VII. Mixed Weighted Sensitivity Minimization

Since the two-bar linkage is a nonlinear system, the frequency response of the inertance model obtained using a subspace identification algorithm is an approximation of the linearized inertance. To account for modeling error, the robustness and tracking performance of the controller are improved by solving a mixed weighted sensitivity problem (see Figure 7).

Let $\Delta_{\rm inrt}(\mathbf{z})$ denote the additive uncertainty in the system dynamics, that is, $G_{\rm inrt}(\mathbf{z}) = \hat{G}_{\rm inrt}(\mathbf{z}) + \Delta_{\rm inrt}(\mathbf{z})$. where $G_{\rm inrt}(\mathbf{z})$ denotes the frequency response of the actual inertance of the system, and $\hat{G}_{\rm inrt}(\mathbf{z})$ denotes the frequency response of the identified inertance model. To account for the frequency-dependent uncertainty, we introduce the model error weighting function $W_{\rm cs}(\mathbf{z})$ such that, for all $\mathbf{z} \in \mathbb{C}$ with $|\mathbf{z}| = 1$, $|\Delta_{\rm inrt}(\mathbf{z})| \leqslant |W_{\rm cs}(\mathbf{z})|$. To improve the tracking performance over the desired bandwidth, we reduce the sensitivity function by introducing a sensitivity weighting function $W_{\rm s}(\mathbf{z})$ that has high gain over this bandwidth. Let $W_{\rm cs}(\mathbf{z})$ and $W_{\rm s}(\mathbf{z})$ have the realizations

$$W_{\rm cs}(\mathbf{z}) \sim \left[\begin{array}{c|c} A_{\rm cs} & B_{\rm cs} \\ \hline C_{\rm cs} & D_{\rm cs} \end{array}\right], \;\; W_{\rm s}(\mathbf{z}) \sim \left[\begin{array}{c|c} A_{\rm s} & B_{\rm s} \\ \hline C_{\rm s} & D_{\rm s} \end{array}\right] \tag{7.1}$$

with states $x_{\rm cs}$ and $x_{\rm s}$, respectively. Next, define the performance variable z by $z \triangleq \begin{bmatrix} z_{\rm s}^{\rm T} & z_{\rm cs}^{\rm T} & (Ru)^{\rm T} \end{bmatrix}^{\rm T}$. where the weighting $R \in \mathbb{R}^{2\times 2}$ on the control input u is positive definite, and $z_{\rm s}$ and $z_{\rm cs}$ are outputs of the transfer functions $W_{\rm s}(z)$ and $W_{\rm cs}(z)$, respectively, such that

$$\begin{aligned} x_{\rm s}(k+1) &= A_{\rm s}x_{\rm s}(k) + B_{\rm s}\left(y_{\rm pos}(k) - r(k)\right), \\ z_{\rm s}(k) &= C_{\rm s}x_{\rm s}(k) + D_{\rm s}\left(y_{\rm pos}(k) - r(k)\right) \end{aligned} \tag{7.2}$$

and

$$\begin{aligned} x_{\rm cs}(k+1) &= A_{\rm cs}x_{\rm cs}(k) + B_{\rm cs}y_{\rm acc}(k), \\ z_{\rm cs}(k) &= C_{\rm cs}x_{\rm cs}(k) + D_{\rm cs}y_{\rm acc}(k). \end{aligned} \tag{7.3}$$

Next, define $w \triangleq \begin{bmatrix} w_{\rm r}^{\rm T} & w_1^{\rm T} & w_2^{\rm T} \end{bmatrix}$, where w_1 and w_2 are fictitious noise signals that facilitate the solution of the estimator Riccati equation for discrete-time LQG synthesis. The plant can then be represented by (3.1)-(3.5), and the state space equations of the standard problem are given by (3.2), with $\tilde{x}$ defined by $\tilde{x} \triangleq \begin{bmatrix} \hat{x}^{\rm T} & x_{\rm s}^{\rm T} & x_{\rm c}^{\rm T} & x_{\rm r}^{\rm T} \end{bmatrix}^{\rm T}$ and

$$\mathcal{A} \triangleq \begin{bmatrix} A_{\rm id} & 0 & 0 & 0 \\ B_{\rm s}\hat{C}_{\rm pos,id} & A_{\rm s} & 0 & -B_{\rm s}C_{\rm r} \\ B_{\rm cs}C_{\rm acc,id} & 0 & A_{\rm cs} & 0 \\ 0 & 0 & 0 & A_{\rm r} \end{bmatrix}, \mathcal{B} \triangleq \begin{bmatrix} B_{\rm id} \\ 0 \\ B_{\rm cs}D_{\rm acc,id} \\ 0 \end{bmatrix}, \tag{7.4}$$

$$\mathcal{D}_1 \triangleq \begin{bmatrix} 0 & D_1 & 0 \\ -B_{\rm s}D_{\rm r} & 0 & 0 \\ 0 & 0 & 0 \\ B_{\rm r} & 0 & 0 \end{bmatrix}, \mathcal{D}_2 \triangleq \begin{bmatrix} 0 & 0 & D_2 \\ D_{\rm r} & 0 & \varepsilon I \end{bmatrix} \tag{7.5}$$

$$\mathcal{E}_1 \triangleq \begin{bmatrix} 0 & C_{\rm s} & 0 & 0 \\ 0 & 0 & C_{\rm cs} & 0 \\ 0 & 0 & 0 & 0 \end{bmatrix}, \; \mathcal{E}_2 \triangleq \begin{bmatrix} D_{\rm s} \\ D_{\rm cs} \\ R \end{bmatrix}, \tag{7.6}$$

$$\mathcal{C} \triangleq \begin{bmatrix} C_{\rm acc,id} & 0 & 0 & 0 \\ 0 & 0 & 0 & C_{\rm r} \end{bmatrix}, \; \mathcal{D} \triangleq \begin{bmatrix} D_{\rm acc,id} \\ 0 \end{bmatrix}. \tag{7.7}$$

The discrete-time LQG problem can now be solved and the controller $G_{\rm c}$ obtained using the procedure discussed in [18]

VIII. Control of a Two-Bar Linkage

The two-bar linkage is stabilized at $\Theta_{1,\rm eq} = -\frac{\pi}{6}$ rad and $\Theta_{2,\rm eq} = -\frac{\pi}{6}$ rad using two PID controllers. The physical parameters of the two-bar linkage are $m_1 = 1$ kg, $m_2 = 2$ kg, $a_1 = 1$ m, and $a_2 = 0.5$ m. The control objective is to have the end effector follow position

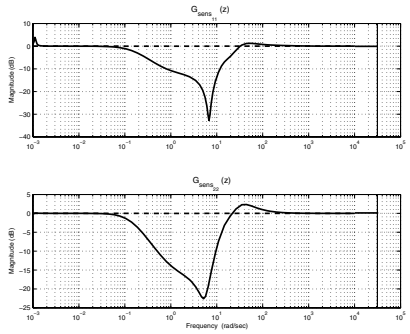

Fig. 8. Magnitude plots of $G_{\mathrm{sens}_{11}}(\mathbf{z})$ and $G_{\mathrm{sens}_{22}}(\mathbf{z})$ before and after mixed weighted sensitivity minimization

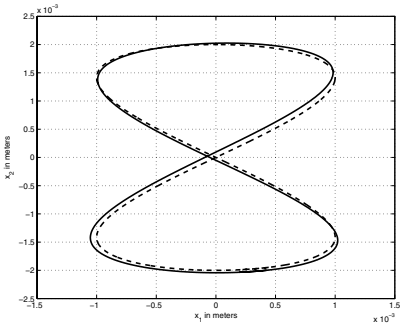

Fig. 9. Position command (dashed lines) and actual path (bold lines) traced by the end effector in the XY plane

commands that are sinusoidal with a spectral bandwidth between 0.01 Hz and 50 Hz. In accordance with this specification, the transfer function $W_{\mathrm{r}}(\mathbf{z})$ is chosen to be $W_{\mathrm{r}}(\mathbf{z}) = \frac{(\mathbf{z}-1)}{(\mathbf{z}-0.999)(\mathbf{z}-0.9999)} I_2$ so that $W_{\mathrm{r}}(\mathbf{z})$ has high gain in the required bandwidth. The controller G_{c} is obtained by the procedure outlined in Section 6. The closed-loop dynamics are analyzed using (5.2)-(5.5) and the magnitude plots of $G_{\mathrm{sens}_{11}}(\mathbf{z})$ and $G_{\mathrm{sens}_{22}}(\mathbf{z})$ defined in (5.4) and (5.5) are shown in Figure 8 by the dashed lines. To reduce the sensitivity over the required bandwidth, the sensitivity weighting $W_{\mathrm{s}}(\mathbf{z})$ is chosen to be $W_{\mathrm{r}}(\mathbf{z})$. To account for the relatively high model uncertainty at high frequencies, the model error weighting function $W_{\mathrm{cs}}(\mathbf{z})$ is chosen to be $W_{\mathrm{cs}}(\mathbf{z}) = \frac{0.2(\mathbf{z}-0.999)}{(\mathbf{z}-0.99)} I_2$. The identified compliance and inertance models are used along with the weighting functions $W_{\mathrm{r}}(\mathbf{z})$, $W_{\mathrm{s}}(\mathbf{z})$, and $W_{\mathrm{cs}}(\mathbf{z})$ to design the LQG controller as described in Section 7. The magnitudes of the diagonal entries of the sensitivity transfer function obtained from mixed weighted sensitivity minimization are shown in Figure 8 by the solid lines.

The nonlinear model of the two-bar linkage is simulated in closed loop with the discrete-time LQG controller using a fourth order Runge-Kutta solver with the sampling time $t_{\mathrm{s}} = 10^{-4}$s. Furthermore, we assume that no process noise acts on the two-bar linkage and that the measurements are not corrupted by noise.The horizontal and vertical position commands for the end effector are sinusoids with amplitudes 0.001 m and 0.002 m and frequencies 6.36 Hz and 3.18 Hz, respectively. Figure 9 shows the position command and actual path traced by the end effector in the XY plane.

IX. Conclusions

In this paper we developed a position-command following controller for a two-bar linkage using acceleration measurements for both system identification and feedback. The method outlined here is applicable to mechanical linkages that have stable or stabilized dynamics. Since a system identification procedure is used to obtain the inertance and compliance models, no modeling information is required. This method is easy to implement because displacement measurements, which are usually difficult to obtain, are not required and a linear controller is used.

References

[1] J. M. McCarthy, *Geometric Design of Linkages*, Springer, 2000.

[2] R. M. Murray, Z. Li, S. S. Sastry, *A Mathematical Introduction to Robotic Manipulation*. CRC Press, Boca Raton, 1994.

[3] J. Wittenburg, *Dynamics of Systems of Rigid Bodies*. Stuttgart, 1977.

[4] F. L. Lewis, C. T. Abdallah and D. M. Dawson, *Control of Robot Manipulators*. Macmillan, 1993.

[5] M. W. Spong and M. Vidyasagar, *Robot Dynamics and Control*. John Wiley and Sons, 1989.

[6] P. S. Krishnaprasad and R. Yang, "On the Geometry and Dynamics of Floating Four Bar Linkages," *Dyn. Stab. Sys.*, vol. 9, pp. 19-45, 1994.

[7] M. Tarokh and H. Seraji, "A Control Scheme for Trajectory Tracking of Robot Manipulators," *Proc. IEEE Conf. Rob. Autom.*, vol. 2, pp. 1192-1197, 1988.

[8] K. Kreutz, "On Manipulator Control by Exact Linearization," *IEEE Trans. Autom. Contr.*, vol. 34, pp. 763-767, 1989.

[9] M. W. Spong and M. Vidyasagar, "Robust Linear Compensator Design for Nonlinear Robotic Control," *IEEE J. Rob. Auto.*, vol. 3, pp. 345-351, 1987.

[10] K. S. Yeung and Y. P. Chen, "A New Controller Design for Manipulators Using the Theory of Variable Structure Systems," *IEEE Trans. Autom. Contr.*, vol. 33, pp. 200-206, 1988.

[11] M. Galicki, "Motion Control of Robotic Manipulators in Task Space," *IEEE Int. Conf. Intell. Rob. Sys.*, vol. 3, pp. 2061-2066, 2002.

[12] J. Y. S. Luh, M. W. Walker and R. P. C. Paul, "Resolved-Acceleration Control of Mechanical Manipulators," *IEEE Trans. Autom. Contr.*, vol. 25, pp. 468-474, 1980.

[13] J. J. Craig, *Adaptive Control of Mechanical Manipulators*. Addison-Wesley, 1988.

[14] M. W. Spong and R. Ortega, "On Adaptive Inverse Dynamics Control of Rigid Robots," *IEEE Trans. Autom. Contr.*, vol. 35, pp. 92-95, 1990.

[15] H. Yazarel and C. C. Cheah,"Task-Space Adaptive Control of Robotic Manipulators With Uncertanties in Gravity Regressor Matrix and Kinematics," *IEEE Trans. Autom. Contr.*, vol. 47, pp. 1580-1585, 2002.

[16] P. Renaud, N. Andreff, G. Gogu, P. Martinet, "On Vision-Based Kinematic Calibaration of n-Leg Parallel Mechanisms," *13th IFAC Symp. Sys. Id.*, pp. 977-982, Rotterdam, 2003.

[17] P. V. Overschee and B. De Moor, "N4SID: Subspace Algorithms for the Identification of Combined Deterministic-Stochastic Systems," *Automatica*, vol. 30, pp. 75-93, 1994.

[18] W. M. Haddad, V. Kapila, E. G. Collins, Jr., "Optimality for Reduced-Order Modeling, Estimation, and Control for Discrete-Time Linear Periodic Plants," *J. Math. Sys. Est. Contr.*, vol. 6, pp. 437-460, 1996.

[19] K. Zhou, J. C. Doyle and K. Glover, *Robust and Optimal Control*. Prentice Hall, 1996.